Pozzi *et al. Herit Sci* (2020) 8:101
https://doi.org/10.1186/s40494-020-00449-1

Heritage Science

RESEARCH ARTICLE Open Access

In search of Humboldt's colors: materials and techniques of a 17th-century lacquered gourd from Colombia

Federica Pozzi[1*], Elena Basso[1*] and Monica Katz[2]

Abstract

In 2014 the Hispanic Society Museum & Library, New York, acquired a viceregal Spanish American lacquered gourd, dating to 17th-century Colombia, which was decorated using an indigenous technique known as *barniz de Pasto*. This technique employs local, raw materials, including natural dyes and a plant resin commonly known as mopa mopa, harvested from *Elaeagia pastoensis* Mora trees that grow in the Andean rainforest. An in-depth scientific study of the gourd aimed at determining its materials and manufacturing techniques, and at comparing the results with the description of local botanical species reported by Alexander von Humboldt, the German naturalist and explorer, in the account of his travels through the region in 1801. The use of several non-invasive techniques was followed by micro-sampling. Initially, X-ray fluorescence (XRF) analysis was performed to evaluate the possible presence of inorganic pigments, while fiber optics reflectance spectroscopy (FORS) and multiband imaging provided preliminary data concerning the colorants. Dyes and pigments were fully characterized using Raman spectroscopy and high-performance liquid chromatography with photodiode array detector (HPLC-PDA); a detailed description of the resin was obtained with HPLC-PDA and pyrolysis-gas chromatography/mass spectrometry (Py-GC/MS); the metallic elements and overall decoration were analyzed by scanning electron microscopy coupled with energy-dispersive X-ray spectroscopy (SEM/EDS). Radiocarbon dating completed the technical information on the object. This work confirmed the identity of the resin as *Elaeagia pastoensis* Mora, supporting an unequivocal classification of the gourd as a *barniz de Pasto* object; the color palette was found to include some of the pigments listed by Humboldt, but also comprised other materials, such as calomel, a rare white pigment based on mercury(I) chloride; examination of the decoration's intricate stratigraphy provided insight into the complexity of the *barniz de Pasto* technique, in which silver leaf is typically applied on top of a sheet of untinted resin and covered with a variable number of dyed resin layers; finally, a pre-1650 date was firmly established for the gourd, which is in line with stylistic observations that had tentatively placed this object in the early *barniz de Pasto* period. In addition to providing conservators with the proper tools to preserve similar lacquered objects, the wealth of knowledge gleaned from this study has revealed fascinating details about the technique employed, demonstrating the extraordinary skill and craftsmanship of the artisans involved in the lacquer arts.

Keywords: Viceregal South America, Gourd, *Barniz de pasto*, Dyes and pigments, Calomel, Silver leaf, Resin, Mopa mopa, *Elaeagia pastoensis*, Lacquer

Introduction

The Hispanic Society Museum & Library (HSML), New York, owns a small group of South American viceregal lacquers, largely acquired in the last three decades, which were created by indigenous artisans for a European aesthetic and meant to imitate Asian lacquers. Within this collection of lacquered artifacts is a gourd purchased in

*Correspondence: federica.pozzi@metmuseum.org; federica.pozzi@metmuseum.org
[1] Department of Scientific Research, The Metropolitan Museum of Art, 1000 Fifth Avenue, New York, NY 10028, USA
Full list of author information is available at the end of the article

2014 (Fig. 1) [1], which was made in the 17th century from a *totuma* or calabash from either *Lagenaria siceraria* or *Crescentia cujete* [2], in Pasto, Colombia. This object is decorated with an indigenous waterproofing and decorative technique called *barniz de Pasto* after its viceregal center of production, which employs local, raw materials including a plant resin and natural dyes, and is still in use today. The resin, commonly known as mopa mopa, comes from harvested leaf buds of *Elaeagia pastoensis* trees (Additional file 1: Figure S1) that grow in the Andean rainforest. In the traditional manufacturing process, the resin was cleaned of plant debris by boiling and chewing; after that, it was dyed, stretched into thin sheets using hands and teeth, and layered with silver leaf to create its iridescent and shiny appearance. The often intricate decorations were then cut out of the dyed sheets, inlaid or layered onto the surface of the object, and typically outlined with black and white pigmented strips of resin (Fig. 2) [3].

Founded in 1539 in the southwestern part of present-day Colombia, Pasto quickly became an administrative, cultural, and religious center. Its location, at 2900 m above sea level, largely intersects with the geographical distribution of the *Elaeagia pastoensis* tree in modern times, which stretches from Costa Rica and Panama in the north to Peru in the south [4]. In the region of Pasto, the *barniz de Pasto* tradition reportedly began under the Spanish influence very early in the viceregal period (1492–1810), and a thriving local craft industry continues to employ the resin today. Further south in Peru, on the other hand, the Inka and their descendants had also been using mopa mopa for over 250 years to decorate wooden ceremonial drinking vessels known as *qeros* [5]. According to Newman and coworkers [6], two species of the genus *Elaeagia*—both growing in these geographical areas—produce copious resin, namely *Elaeagia pastoensis* L. E. Mora [7] and *Elaeagia utilis* (Goudot) Wedd. While the first was typically used for artifacts manufactured in Pasto, the latter was mostly employed in Andean *qeros* produced by Inkas, and continued to be used by the indigenous populations during the viceregal and modern periods. Early research on Inka and viceregal *qeros* (as well as viceregal objects from Colombia and Ecuador) before Newman's work had identified mopa mopa resin in various artifacts [5], but had been unable to differentiate between the two species of resin-producing *Elaeagia*, leading to assumptions that the two traditions were related. However, while it cannot be discounted that the Pasto artisans had knowledge of the Peruvian *qeros*, it now appears unlikely that the *barniz de Pasto* tradition evolved directly from that of *qeros* [8].

In the viceregal period two different techniques using *Elaeagia pastoensis* evolved contemporaneously: *barniz brillante*, found on the gourd in this study and characterized by a glittering appearance, and *matte barniz*, which employs pigment-saturated, matte resin to decorate similar objects as *barniz brillante*, such as boxes, caskets, portable desks, and table-tops. Although there are references in early chronicles to objects that may have been decorated with colored resin [9], the first mention of artisans in Pasto was in 1676 by Lucas de Piedrahita [10], a Roman Catholic prelate who served as the Bishop of Panamá, who noted that the artifacts produced were already "*prized in these parts of Europe*", with reference to Spain. Dating of the HSML *barniz de Pasto* collection has assumed that, based on Piedrahita's account, the earliest objects cannot be vouchsafed a date before ca. 1650—accounting for a generation to allow for the fame of the

Fig. 1 Gourd vase (*barniz de Pasto*). Pasto, Colombia, 17th century. Lacquer, *barniz de Pasto*, H 12 cm, LS2400. Courtesy of The Hispanic Society of America, New York

Fig. 2 Micrographs of four details from the gourd's intricate decoration, showing two owls, a flower, a bird, and a unicorn inlaid onto the object's surface and outlined with black and white pigments

craft to reach Europe. In addition, it has been observed that earlier artifacts in the HSML collection incorporate a more intricate decoration and iconography from early modern illuminated manuscripts, while later pieces, on the other hand, tend to include more generic and simpler flora and fauna, displaying a design that is more evidently imitative of Asian lacquer (Codding M, Personal communication with author MK, 2019). In this context, the elaborate decoration of the gourd investigated in this study, which combines local flora and fauna with mythical creatures such as griffins and unicorns from early modern Books of Hours, seems to be consistent with what is observed in the earlier period of the *barniz de Pasto* tradition.

Among the rare written sources regarding the *barniz de Pasto* technique [10–13], the best known account was compiled by Alexander von Humboldt, German explorer and naturalist who travelled through the region, from Cartagena to Lima, at the end of 1801 [14]. During his expedition, Humboldt researched and named the locally-available pigments and colorants that he believed were used in the production of *barniz de Pasto* objects, also describing a thriving cottage industry, and reporting an unsubstantiated origin story for this art form that allegedly dated to the beginning of the 17th century.

Despite an undeniably growing interest and fascination with South American art, recently resulting in an increasing number of technical studies on this topic [15–28], scientific investigations of *barniz de Pasto* are still limited, while more information can be found on related decorative techniques. An article published in 1992 by Portell [29] reports two Fourier-transform infrared (FTIR) spectra of blue and green glazes from a polychrome wooden statue of the Immaculate Conception created in Quito using *barniz chinesco*, a technique in which gold and silver leaf were extensively applied together with transparent glaze layers to walls and ceilings of churches as well as free-standing figures. In that work, the identification of Prussian blue and copper resinate in such glazes is accompanied by a commentary describing *barniz de*

Pasto alongside similar techniques used in Latin America during the viceregal period, and only a brief reference is made to scientific analyses that were reportedly in progress at the time of publication. Another paper by Pearlstein and coworkers [5] describes the preliminary results of a technical survey of 150 *qeros* from four museum collections, aiming to investigate their constituting materials and methods of manufacture. Visual examination followed by analysis with polarized light microscopy, electron microprobe spectroscopy, FTIR, and gas chromatography/mass spectrometry (GC/MS) provided insight on wood identification and found the *qeros*' decoration to be mostly composed of mopa mopa resin with orpiment, cinnabar, a few unidentified organic reds, lead white, indigo, and copper-based greens. A subsequent publication by a team including the same authors [30] explores the occurrence of a titanium dioxide/silica white pigment on 12 wooden Andean *qeros*, characterized by X-ray diffraction (XRD), X-ray fluorescence (XRF), and Raman spectroscopy as mainly consisting of cristobalite, anatase, and α-quartz. Another article by Newman and Derrick [31] focuses on the identification of mineral pigments, synthetic inorganic compounds, and natural dyestuffs in a number of paint samples removed from *qero* cups in the holdings of four museums across the United States. Furthermore, the results published by Curley and coworkers, presenting the isotopic composition of lead white pigments, have suggested the possibility of being able to identify chronology and production centers from pigment use on *qeros* [32]. In 2015, Newman and coworkers published a comprehensive study of resins from *Elaeagia pastoensis* and *Elaeagia utilis* species, with a special focus on the possibility of differentiating between them analytically [6]. Analysis with FTIR, pyrolysis-GC/MS (Py-GC/MS), and high-performance liquid chromatography with photodiode array and mass spectrometer detectors (HPLC-PDA-MS) was carried out on 19 herbarium specimens of resin, and results were then compared with data acquired from samples of inlays removed from objects made during the viceregal period in Pasto and from viceregal Inka *qeros*. One of the most significant technical studies of *barniz de Pasto* objects reported in the literature was recently presented in an article by Burgio and coauthors [33]. Their work investigates the materials and techniques employed in the manufacture of a rare table cabinet decorated with *matte barniz* in the collection of the Victoria and Albert Museum (London, UK), using, among other techniques, XRF, XRD, FTIR, Raman spectroscopy, scanning electron microscopy coupled with energy-dispersive X-ray spectroscopy (SEM/EDS), and micro-computed X-ray tomography. While in this case characterization of the resin as mopa mopa relied merely on FTIR analysis, the discussion of pigments found on the object mostly focused on the rare discovery of mercury(I) chloride, or calomel, used deliberately as a white pigment.

In this context, an in-depth analytical study of the HSML lacquered gourd was undertaken with four main goals: first, to identify the resin and, thus, provide scientific evidence to support an unequivocal classification of the gourd as a *barniz de Pasto* object; second, to characterize the pigments and colorants, and compare the results with Humboldt's description of local botanical species; third, to examine the stratigraphy of the decoration and gain insight into the complexity of the *barniz de Pasto* technique; and fourth, to date the object precisely in an attempt to verify an extant theory according to which pre-1650 pieces incorporate iconography from early modern manuscripts, while in later objects simpler flora and fauna dominated the decoration. In addition to providing conservators with the proper tools to preserve similar lacquered objects for future generations, the wealth of knowledge gleaned from this study represents a valuable addition to the existing body of literature, revealing in detail, for the first time, the extraordinary skill and craftsmanship of the artisans involved in the lacquer arts.

Experimental

The extensive campaign of scientific analysis performed on the HSML gourd relied on a multi-technique approach involving non-invasive and micro-invasive techniques, the removal of samples (Table 1), as well as the use of portable instruments for in-situ analysis and benchtop equipment located in the Department of Scientific Research (DSR) of The Metropolitan Museum of Art (The Met). Initially, non-invasive XRF analysis was carried out at the HSML conservation laboratory using a portable spectrometer to gain preliminary information on the possible presence of inorganic materials on the gourd. After that, the object was transferred to The Met for further non-invasive investigations by means of a micro-XRF (μXRF) system, X-radiography, multiband imaging, fiber optics reflectance spectroscopy (FORS), and Raman spectroscopy. While the gourd was in overall good state of preservation, seven microscopic scrapings and multi-layered samples for cross sections were removed from disrupted areas and pre-existing losses. Samples were photographed under polarized and ultraviolet (UV) light; then, they were analyzed by surface-enhanced Raman spectroscopy (SERS), HPLC-PDA, and SEM/EDS, with the main goals to provide an unambiguous identification of the pigments and colorants, and to offer insight into the complex decoration of the gourd. Scrapings were also investigated with HPLC-PDA and Py-GC/MS to afford a detailed characterization of

Table 1 List of microscopic samples removed from the HSML gourd with corresponding descriptions and sampling sites

Sample	Description	Location
S1	Cross section of green decoration	Area of green background on outer neck, where edge is broken and part of decoration has detached
S2	Cross section and scraping of red decoration	Area of red border on inner neck, where edge is broken and part of decoration has detached
S3	Cross section of golden decoration	Area of golden and blue triangles on inner neck, where edge is broken and part of decoration has detached
S4	Cross section and scraping of yellow decoration	Area of yellow leaf near unicorn figure, where a small part of decoration has detached
S5	Fragment of untinted resin	Area of untinted resin on interior along fracture, where part of resin has detached
S6	Cross section of silver-white decoration	Area of silver-white moon on red band along fracture
S7	Fragment of bare gourd	Area of bare gourd on neck, where edge is broken and decoration has detached

the resin. In addition, a small fragment of bare gourd, removed from a broken corner where the decoration had detached, was sent to the Accelerator Mass Spectrometry Laboratory, University of Arizona (Tucson, Arizona), for radiocarbon dating. Experimental conditions for the analytical techniques used are reported in the following section.

XRF Analysis was performed using an Elio XGLab energy-dispersive portable XRF spectrometer, with a high-resolution large-area silicon drift detector (SDD) with 130 eV at manganese (Mn) Kα with 10 kcps input photon rate (high-resolution mode), and 170 eV at MnKα with 200 kcps input photon rate (fast mode). The system is equipped with changeable filters, and a rhodium (Rh) transmission target with 50-kV maximum voltage and 4-W maximum power. The size of the spot analyzed was 1 mm. Parameters employed for the analysis were 50-kV voltage, 60-μA current, 120-s acquisition time, and no filter. Further analysis at higher resolution were conducted by means of an open-architecture Bruker Artax μXRF spectrometer equipped with a 0.2-mm collimator, using unfiltered Rh radiation at 50 kV, 700 μA, and acquiring each spectrum for 240 s in air.

X-radiography Computed radiography was carried out using a Phillips MG321 X-ray system as a source and a Carestream HPX-1 CR system with an $8'' \times 10''$ Kodak Industrex Flex HR digital plate for digital capture. Two exposures were made with aluminum primary-beam filter removed, with a target-to-imaging-plate distance of 90 cm. Exposure HSML-LS2400(20190521XR)001 was taken at 25 kV and 5 mA for 30 s. Exposure HSML-LS2400(20190521XR)002 was taken at 16 kV and 4 mA for 30 s. The captured images were processed using a proprietary Carestream number 2 edge filter. Exposure 002 was adjusted for brightness (+0.3).

Multiband imaging All images were acquired with a Nikon D90 modified DSLR camera equipped with a UV-Vis-IR 60 mm 1:4 APO macro lens. For infrared reflected (IRR) images, a Peca 910 filter was used; collection of ultraviolet reflected (UVR) images employed a Peca 900 and a Xnite BP1 filter; visible images were recorded by means of a IDAS-UIBAR filter. IR and UV reflectance false color (IRRFC and UVRFC) images were obtained by transferring individual color channel image data (red, green, and blue channels, RGB) into a yellow/magenta/cyan system in Photoshop. Specifically, IRRFC images were produced by transferring the green and red channels of the visible image into yellow and magenta, respectively, while the cyan channel was substituted with the IRR image; and UVRFC images were created by transferring the blue and green channels of the visible image into cyan and magenta, respectively, whereas the yellow channel was substituted with the recolored UVR monochrome image.

FORS Analysis was performed using an Ocean Optics (USB2000 + UV/Vis) spectrometer equipped with a linear silicon charge-coupled device (CCD) array. In this system, the area selected for analysis is illuminated through a halogen lamp coupled with fiber optics. Reflected light is collected by a co-axial fiber and driven to the spectrometer. Analysis was carried out by positioning the tip of the fiber optics at approximately 1–2 mm from the object's surface, resulting in a spot size of approximately 0.2 mm. Reflectance (R) data were converted to apparent absorption using the Kubelka–Munk algorithm, as the positions of the absorption features are considered to be more constant and maxima are more informative [34].

Raman Analysis was conducted using a Bruker Senterra Raman spectrometer equipped with an Olympus 50× long working distance microscope objective and a CCD detector. A continuous wave diode laser, emitting light at 785 nm, was employed as the excitation source, and two holographic gratings (1800 and 1200 rulings/mm) provided a spectral resolution of 3–5 cm^{-1}. The output laser power was kept below 10 mW, while the number of scans and integration time were adjusted to

prevent damage from overheating and according to the Raman response of the areas examined. Spectra were interpreted by comparison with published literature and library databases available at The Met's DSR.

SERS Analysis was carried out using the same instrument described above, in association with a Spectra Physics Cyan solid state laser that provided excitation at 488 nm. Two pretreatment methods have been applied consecutively on the same sample, in order to induce hydrolysis of the dye-mordant complex bonds of the lake pigments possibly present according to their chemical class [35, 36]. In detail, each sample was initially treated with 0.6 µL of 1% nitric acid, which hydrolyzes the dye-mordant complex and, at the same time, prompts aggregation of the silver (Ag) nanoparticles. After that, samples were covered with a 2-µL drop of Ag colloid and SERS spectra were thus acquired. Upon rinsing, samples were exposed to hydrofluoric acid vapor in a polyethylene micro-chamber for 5 min and then covered with a 2-µL drop of Ag colloid, followed by 0.5 µL of 0.5 M potassium nitrate as aggregating agent. Ag nanoparticles were prepared by microwave-supported glucose reduction of silver sulfate in the presence of sodium citrate as a capping agent, according to a procedure previously published [37]. Output laser powers below 0.4 mW were employed for the analysis, with two integrations of 15 s.

SEM/EDS Analysis was performed with a FE-SEM Zeiss Σigma HD system equipped with an Oxford Instrument X-MaxN 80 SDD. Back-scattered electron (BSE) imaging, as well as EDS elemental spot analysis and mapping, were performed in high vacuum at 20 kV, on 12-nm carbon-coated samples.

HPLC-PDA Samples from the gourd were placed in reactivials, soaked in 5–6 µL of a mixture of 10% boron trifluoride (BF_3) and methanol (2/3, v/v), stirred on a Vortex, ultrasonicated for 5 min, then left at room temperature overnight. 50 µL of BF_3 and methanol extracting solution were then added to the reactivials and evaporated under a gentle N_2 stream twice. The dye extracts were recovered in 11 µL of methanol and 11 µL of 1% aqueous formic acid (v/v). Each solution was filtered, centrifuged for 5 min at 3500*g*, and the supernatant thus injected into the HPLC system [38]. The analytical system used consisted of a 1525 micro binary HPLC pump, 1500 series column heater, in-line degasser, and a Rheodyne 7725i manual injector with 20-µL loop (Waters Corporation, Milford, Massachusetts). An XBridge BEH Shield RP18 reverse-phase column (3.5-µm particle, 2.1-mm I.D. × 150 mm) equipped with an XBridge BEH Shield RP18 guard column (3.5-µm particle, 2.1-mm I.D. × 5 mm, Waters Corporation, Milford, Massachusetts) was used with a flow rate of 0.2 mL/min. An Upchurch ultra-low volume pre-column filter with a 0.5-µm stainless steel frit (Sigma-Aldrich, St. Louis, Missouri) was attached in front of the guard column. The column temperature was set to 40°C. The mobile phase was eluted in a gradient mode of (A) 1% formic acid in deionized water (v/v) and (B) a mixture of methanol and acetonitrile (1/1, v/v). The solvent gradient was as follows: 90% (A) for 3 min, 90–60% (A) in 7 min in a linear slope, 60–0% (A) in 24 min in a linear slope, 0–90% (A) in 1 min, then held at 90% (A) for 10 min. A 2996 PDA detector was employed to obtain spectral information in the 210–800 nm range. Operation and data processing were performed using Empower Pro software (2002).

Py-GC/MS Analysis was conducted on an Agilent 5973N gas chromatograph equipped with a Frontier PY-2020iD Double-Shot vertical furnace pyrolyzer fitted with an AS-1020E Auto-Shot autosampler. The GC was coupled to a 5973N single quadrupole mass selective detector (MSD). Samples of 60–70 µg were weighed out in deactivated pyrolysis sample cups (PY1-EC80F Disposable Eco-Cup LF) on a Mettler Toledo UMX2 Ultra microbalance, and then derivatized with tetramethyl ammonium hydroxide (TMAH) before pyrolysis. Derivatization took place in the same cups as follows: 3.5 µL of 25% TMAH in methanol (both from Fisher Scientific) were added directly to the sample in each cup with a 10-µL syringe and, after 2 min, loaded onto the autosampler [39]. The interface to the GC was held at 320°C and purged with helium for 30 s before opening the valve to the GC column. The samples were then dropped into the furnace and pyrolyzed at 550°C for 30 s. The pyrolysis products were transferred directly to a DB-5MS capillary column (30 m × 0.25 mm × 1 µm) with the helium carrier gas set to a constant linear velocity of 1.5 mL/min. Injection with a 20:1 split was used, in accordance with the instrument's recent performances and the sample size. The GC oven temperature program was: 40°C for 1 min; 10°C/min to 320°C; isothermal for 1 min. The Agilent 5973N MSD conditions were set as follows: transfer line at 320°C, MS Quad 150°C, MS Source 230°C, electron multiplier at approximately 1770 V; scan range 33–550 amu. As samples were derivatized with TMAH, the detector was turned off until 4 min to avoid saturation by excess of derivatizing agent and solvent. Data analysis was performed on an Agilent MSD ChemStation D.02.00.275 software by comparison with the NIST 2005 spectral libraries and available literature.

Preparation of cross sections Cross sections were prepared by embedding each sample within a double layer of methyl methacrylate resin (Technovit® 2000 LC). Each layer of resin was cured under UV light for 20 min. Excess resin was ground off and surface was finely polished using CarbiMet 2 and Micro-mesh abrasive paper of various grits to expose the samples' stratigraphy.

Results and discussion

Resin

Identification of the resin was achieved by removing a sample of untinted material from the interior of the HSML gourd (S5), followed by analysis with HPLC-PDA and Py-GC/MS. These results were then compared with literature data and with those obtained from the investigation of two reference samples of raw and boiled *Elaeagia pastoensis* resin. The first of these reference samples (raw resin) was a gift from the *barniz de Pasto* workshop of Gilberto and Oscar Granja in Pasto, which one of the authors visited in 2011; it was broken from a brick of unprocessed resin, destined to be colored and used in the decoration of a modern object. The second (boiled resin), collected in 2012 and subjected to repeated boiling, was provided by Emily Kaplan, Objects Conservator at the Smithsonian National Museum of the American Indian (NMAI).

The HPLC-PDA chromatograms acquired from the two references of *Elaeagia pastoensis* resin displayed slightly different profiles in terms of their relative abundance of detected compounds, which is likely attributable to the different manufacturing process undergone by the two materials upon harvesting (none vs. boiling). The most characteristic molecules found in both reference samples include two widely occurring natural flavones, luteolin (16.11 min) and apigenin (17.88 min), as well as luteolin monomethylether or related derivative (17.66 min) (Fig. 3b). The series of compounds identified in the two reference resins, along with their observed distribution, are consistent with HPLC-PDA-MS results previously reported by Newman and coauthors for *Elaeagia pastoensis* species [6]. According to their study, the distinction between specimens from *Elaeagia pastoensis* and *Elaeagia utilis* may rely on the detection of a few additional components in chromatograms of the latter that are not present in the former, namely quercitin, kaempferol, and the monomethyl ether of apigenin. Data collected from sample S5 show an excellent correspondence to those obtained for the reference of *Elaeagia pastoensis* boiled resin (Fig. 3), both in terms of the series of characteristic components detected and the relative amounts observed, and are consistent with the results reported in Newman's article for samples from this plant species.

Similarly to what was observed for HPLC-PDA, when analyzed with Py-GC/MS, the two references of *Elaeagia pastoensis* resin were found to contain the same series of distinctive compounds in different relative amounts, which, as stated above, might be due to the different manufacturing process undergone by the two materials upon harvesting (none vs. boiling). Upon derivatization, organic compounds containing acidic functional groups in the sample, such as carboxylic acids, alcohols, and phenolic compounds, are deprotonated by the alkaline TMAH and the resulting tetramethylammonium salts are thermally converted to the corresponding methyl esters in the hot injection port of the gas chromatograph. The most characteristic molecules found in the two references examined here include: glycerol derivatives (8–8.5 min), along with various fatty acids, mainly stearic (23.36 min), palmitic (21.52 min), and azelaic (17.48 min); several compounds containing a single aromatic group (15.5–18 min), including methyl ester of 3,4-dimethoxybenzoic acid, 1-(3,4-dimethoxyphenyl)ethanone, 1,2-dimethoxy-4-(1-propenyl)-benzene, 3,4-dimethoxybenzaldehyde, methyl ester of azelaaldehydic acid, 1,3,5-trimethoxybenzene, and 4-ethenyl-1,2-dimethoxybenzene; two cinnamic acid derivatives, i.e. methyl *p*-methoxycinnamate (19.01 min) and methyl 3,4-dimethoxycinnamate (21.14 min); a series of unidentified, but recurrent compounds (24–28 min); the dimethyl ether (29.71 min) and trimethyl ether (31.05 min) of the flavonoid apigenin, as well as the tetramethyl ether of the flavonoid luteolin (32.68 min); and numerous pentacyclic triterpenoids (30–40 min) (Fig. 4b). The series of compounds detected in the two reference resins and their observed distribution are consistent with Py-GC/MS data previously reported for *Elaeagia pastoensis* species by Newman and coauthors [6]. Their work shows that Py-GC/MS chromatograms of *Elaeagia utilis* specimens contain similar components as *Elaeagia pastoensis*, albeit in different relative amounts. Notably, two of the unidentified

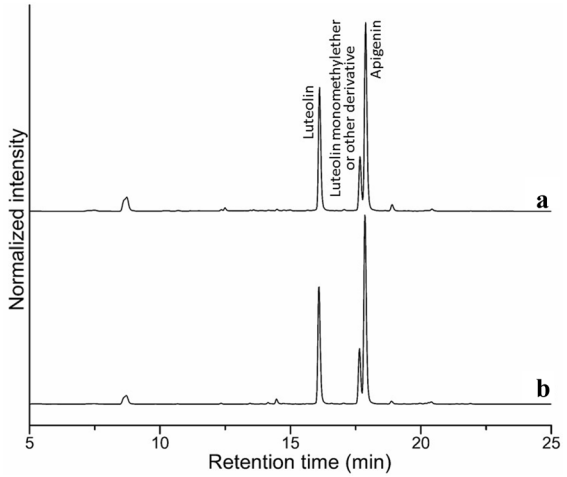

Fig. 3 **a** HPLC-PDA chromatogram at λ = 350 nm obtained upon extraction in 4% BF_3 in MeOH of sample S5, i.e. a small chip of untinted resin from the interior of the gourd, compared with **b** a chromatogram acquired in the same conditions from a reference sample of *Elaeagia pastoensis* boiled resin. Compounds identified in both chromatograms include luteolin, apigenin, and luteolin monomethylether or related derivative

compounds eluting, in this case, between 24 and 28 min, are reported to have been consistently found in *Elaeagia pastoensis* samples, but only rarely in *Elaeagia utilis* species, and can therefore be used as markers. The detection of the latter molecules in the current analysis, along with the observed overall distribution of marker compounds, confirms that the two reference resins analyzed belong in fact to the *Elaeagia pastoensis* species. The chromatogram obtained from sample S5, dominated by an intense peak of methyl 3,4-dimethoxycinnamate, is consistent with that of the reference of *Elaeagia pastoensis* boiled resin (Fig. 4), both in terms of the series of distinctive compounds detected and their relative amounts, and concurs with data previously reported by Newman for samples from this plant species.

The combined results of HPLC-PDA and Py-GC/MS analysis conclusively confirmed the use of *barniz de Pasto* to decorate the gourd, further corroborating the previous classification based on visual examination and stylistic considerations. Despite many descriptions of mopa mopa in its raw state being greenish-yellow [6, 40, 41], the resin used on the interior of the gourd appears reddish-brown, which is a common feature to all the *barniz de Pasto* objects in the HSML collection. Chromatographic analyses have shown that no other colorants are present at the sampling location aside from a series of flavonoids that are inherent to the resin's composition itself. Therefore,

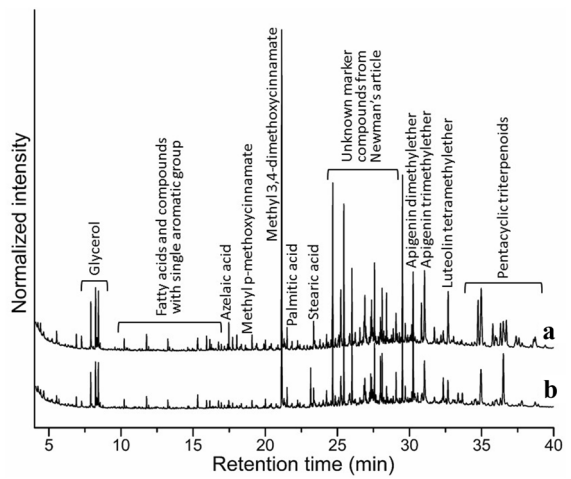

Fig. 4 **a** Py-GC/MS chromatogram obtained upon derivatization with TMAH of sample S5, i.e. a small chip of untinted resin from the gourd's interior, compared with **b** a chromatogram acquired in the same conditions from a reference sample of *Elaeagia pastoensis* boiled resin. Compounds identified in both chromatograms include glycerol derivatives along with various fatty acids, several molecules containing a single aromatic group, two cinnamic acid derivatives, a series of unidentified but characteristic compounds, the dimethyl and trimethyl ethers of apigenin, as well as the tetramethyl ether of luteolin, and numerous pentacyclic triterpenoids

a possible explanation for the observed color may lie in the fact that the layer of resin applied to the interior of the gourd is approximately 1-mm thick, i.e. significantly thicker than the resin used on the outer decoration, and laid directly onto the brownish gourd substrate. The resin found on the exterior, on the other hand, is typically no more than a few microns thick and laid on top of a silver leaf, which may account for its transparency and light reflectivity.

Pigments and colorants

The gourd has a limited palette of translucent colors over metal leaf: green is found in the background; red, pink, yellow, gold, and blue dominate the decoration's flora and fauna; while saturated white, cream, and black are used as outlines of the decorative elements. In his account, Humboldt described the colors employed in *barniz de Pasto* objects as dilute indigo for blue; pure indigo for black; achiote, a dye derived from *Bixa orellana* seeds, for red; the powdered extract of *Escobedia scabrifolia*, a saffron-like root, over silver leaf for gold; and lead oxide for white [14]. In the present study, characterization of the pigments and colorants was mostly expected to confirm the presence of those locally available described by Humboldt. It is also worth noting that a key feature of the mopa mopa resin is its waterproof nature, as well as the remarkable physical changes it undergoes from a pliable and elastic substance capable of being stretched into translucent sheets to the shiny, rigid, and impermeable finish observed on the surface of the gourd. The intrinsic hardness of the resinous matrix in its final form [6] might be one of the reasons why identification of the colorants embedded in it has posed a longstanding challenge, and the few attempts commissioned from external laboratories by the HSML prior to this study failed (Newman R, Unpublished report, 2015).

As expected, in-situ XRF measurements ubiquitously detected silver, used in the gourd's metal leaf, but yielded no results on the colored areas, most of which, indeed, were believed to be made of organic dyes. In addition, XRF spectra displayed surprising mercury peaks, along with chlorine, at several locations; this observation could be explained by the findings in Burgio's 2018 publication [33], in which the authors report on their discovery of mercury(I) chloride (Hg_2Cl_2), or calomel, deliberately employed as a white pigment on a 17th-century *barniz de Pasto* box in the collection of the Victoria and Albert Museum. Our initial analysis with a portable system was subsequently refined by using μXRF to avoid interference from adjacent regions and precisely locate mercury and chlorine in the incredibly detailed decorations of the gourd (Fig. 5a). The presence of calomel, inferred by XRF in all the object's saturated white details, flora and

fauna outlines, and in the silver-white crescent moons that frame the decoration quadrants, was unambiguously confirmed by Raman spectroscopy due to the detection of distinctive bands at 167 and 275 cm^{-1} (Fig. 5b) [33].

Calomel, naturally formed from the alteration of other mercury-containing mineral ores such as cinnabar (HgS) upon reaction with chlorine in the atmosphere or in chorine-rich soils [42–48], has been known as an ingredient in medications and cosmetics [49–51]. However, it can also be manufactured artificially. A method of production known for centuries and reported in a 19th-century study of Japanese pigments involves sublimation of a pulverized mixture of alum, mercury, and common salt in a furnace [52]. Albeit produced in China prior to the 10th century, only in the first half of the 16th century did this compound become known to the Western world [53], where it started to be manufactured, likely in England, in the mid-17th century [54]. Deposits of cinnabar, a natural precursor of calomel, are widespread in Central and South America, and their exploitation dates back to prehistoric times [55]. Intensive mercury mining in the New World first began ca. 1400 B.C.E., predating the emergence of complex Andean societies, and the earliest activity targeted cinnabar for the production of vermilion [56]. This practice strongly increased under the Spanish colonial government, when the use of the mercury amalgamation technology for the extraction of gold and silver reached its acme [57, 58]. Nowadays, the Nariño province, where Pasto is located, is still one of the most important regions for gold and silver mining. Although 45 cinnabar deposits have been recently inventoried in Colombia [59], little is known about which ones were exploited by pre-Hispanic cultures [55, 60]. Based on the available documentary sources, it cannot be ruled out that cinnabar exploitation to produce mercury for gold and silver mining in Colombia may have begun under the Spanish government. If this hypothesis is confirmed, the possibility that natural calomel may have been employed for the HSML gourd would be as viable as the use of an artificially produced material.

Whites commonly used in South American artifacts have ranged from calcium-containing minerals, such as calcite, gypsum, and apatite [61–64], to lead white [65]. Similarly, scientific analysis carried out to date on *qero* cups has highlighted a predominant use of lead white in the form of hydrocerussite (basic lead carbonate, $2PbCO_3{\cdot}Pb(OH)_2$) and cerussite (neutral lead carbonate, $PbCO_3$) [5, 6], along with a naturally-occurring mixture of cristobalite (SiO_2), anatase (TiO_2), and α-quartz (SiO_2) [30, 66]. In the collection of the HSML, lead white was detected in a *barniz de Pasto* box dating to 1684 (Newman R, Unpublished report, 2015), and this finding appeared to support Humboldt's description of white in *barniz de Pasto* objects as "*made imperfectly with white lead oxide*" [14]. In the past year, however, calomel was also identified by the authors on two *barniz de Pasto* caskets dated to 1650 and 1700 in the HSML holdings (Pozzi F and Basso E, Unpublished report, 2019), and similar results were obtained by scientists at the Fitzwilliam Museum (Cambridge, UK) from the analysis of a 15th-century illuminated manuscript and a late 16th-century portrait miniature [67]. Before Burgio's work, calomel was never reported as a pigment in cultural heritage objects. In addition to substantiating her initial finding of calomel as an intentionally used white pigment, such recent discoveries clearly indicate that this material was more commonly employed in works of art and cultural heritage objects than initially thought.

Red was an important color both to European and pre-invasion indigenous cultures [68], and, in the region of Pasto, several mineral and botanical sources could yield an intense red hue. Among the red pigments historically available in South America, cinnabar had been used extensively as face and body paint by the Inkas, for ceramics, as well as in Inka *qeros* [24, 26, 69]. Similar shades of red could be also produced from certain indigenous dyes, such as cochineal, obtained from female insects of the *Dactylopius coccus* Costa species, and achiote, extracted from the seeds of the *Bixa orellana* plant [70]. In his account, Humboldt described the red in *barniz de Pasto* objects as "*derived from Urucu* (*Bixa orellana, mixed with rubber milk*) *powder*" [14]. Initial XRF analysis of the HSML gourd's red decoration revealed only trace amounts of mercury, leading the authors to rule out a widespread presence of cinnabar. Further testing with FORS, yielding spectra characterized by apparent absorbance maxima at 520 and 560 nm (Fig. 6a), immediately suggested the possible use of an organic red of animal origin [71]. While SERS of a microscopic sample removed from the object's inner neck (S2) failed, likely due to the interference of the thick mopa mopa layer in which the dye is embedded, extraction with BF_3 and methanol followed by HPLC-PDA analysis enabled the conclusive identification of carminic acid—the main coloring component of cochineal—and some of its methylated derivatives (Additional file 2: Figure S2). This dye, also found by other researchers in a selection of Andean *qeros* [30, 31], was particularly popular in the 16th and 17th centuries, becoming the third most profitable traded commodity from the New World for the Spanish after silver and gold, and displacing kermes as the source of luxurious crimson and scarlet textiles within 50 years of its introduction [65]. Called *grana* by the Spanish, it had been cultivated on *Opuntia cacti* from about 600 C.E. by the indigenous populations, who had developed a sophisticated dyeing process with it, to the

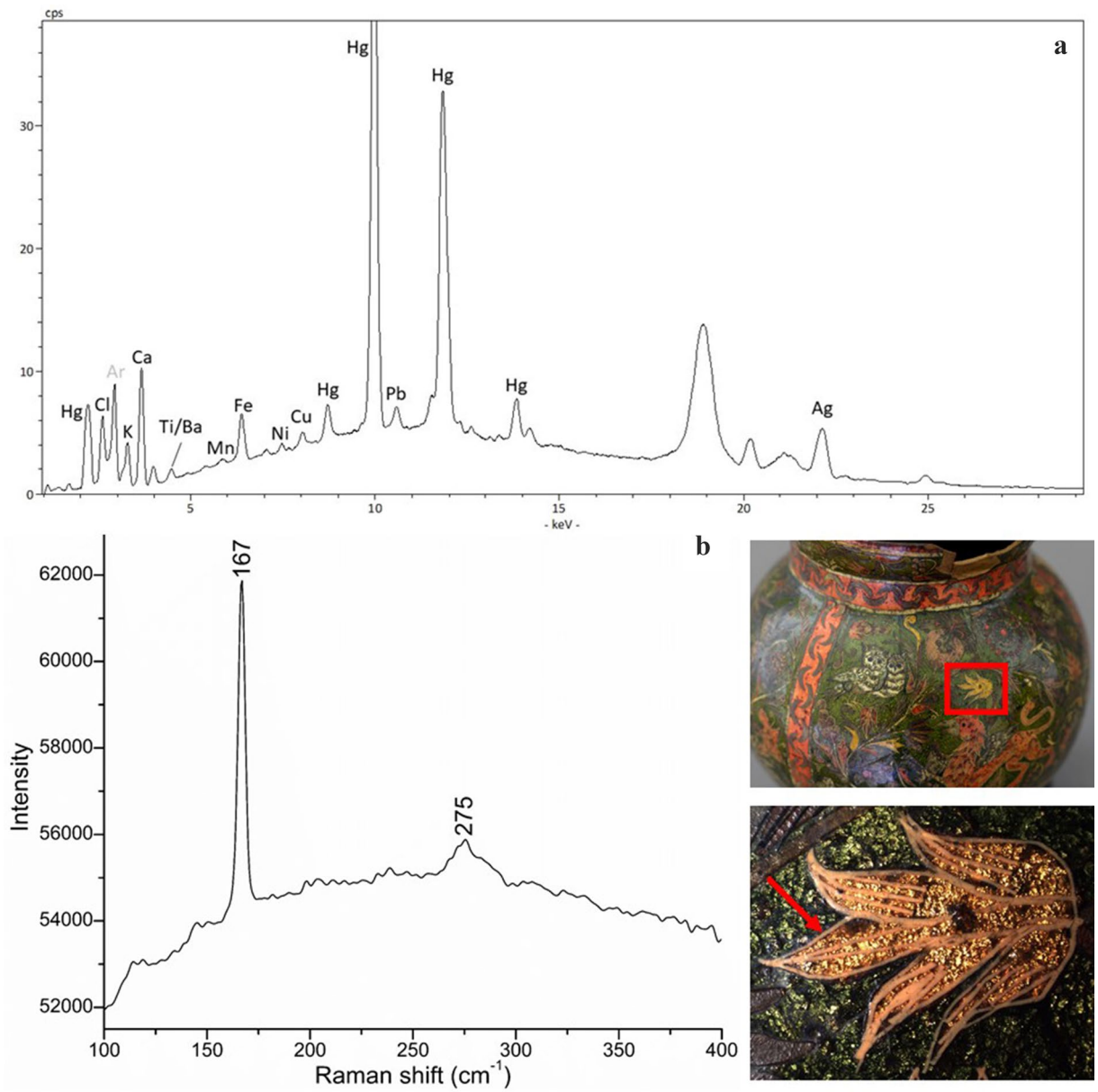

Fig. 5 **a** XRF spectrum acquired from the gourd's white decoration outlines, displaying prominent mercury (Hg) peaks from calomel and silver (Ag) peaks from the underlying silver leaf. **b** Raman spectrum collected from the same area, revealing the characteristic bands of calomel at 167 and 275 cm^{-1}. The area analyzed is marked in the object image with a red rectangle and arrow

point that the many shades of red derived from cochineal are each identified by name in the contemporary chronicles [69, 72, 73].

Humboldt's account of the yellow and gold found on *barniz de Pasto* objects states: "*Yellow is derived from the powdered root of the Escobedia Flor. Per. or from saffron from the earth. Gold is also made from Escobedia applied on top of a silver leaf*" [14]. He believed the colorant to be obtained from *Escobedia scabrifolia*, a locally grown saffron-like root that is still used today in Colombian cuisine to color foods and drinks [74]. Yellow dyes are among the most difficult cultural heritage materials to characterize analytically, mostly due to the lack of adequate spectral databases to be used in identification studies and the fact that hundreds of plants can produce yellow extracts [75–77]. As observed in the case of red areas, XRF spectra acquired from yellow and golden portions of the decoration did not display any elements that could indicate

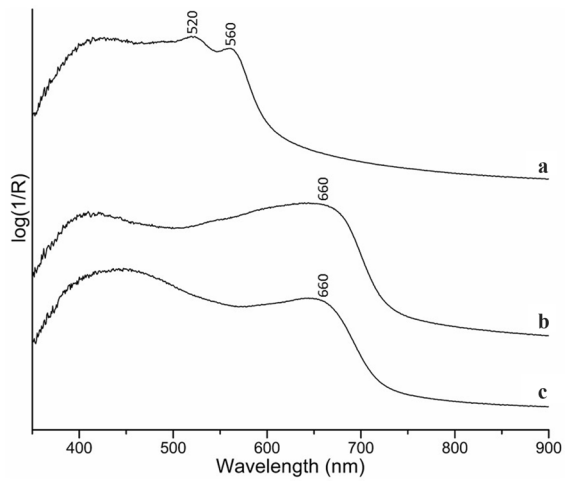

Fig. 6 **a** FORS spectrum of a red area from the gourd, in which apparent absorbance maxima at 520 and 560 nm suggest the possible use of an organic red of animal origin. **b**, **c** FORS spectra of blue and green areas from the gourd, in which an apparent absorbance maximum at 660 nm suggests the possible presence of indigotin

the presence of inorganic pigments such as, for example, orpiment. The organic nature of these colorants was further supported by UVRFC imaging of the object (Fig. 7a), in which all yellow dyes typically show as red [78–80]. From an analytical standpoint, FORS is generally not suitable to characterize yellow colorants, as their spectra appear broad and featureless, while SERS, again, yielded no results due to the hard texture of the embedding resin, thus interfering with the analysis. At first glance, the HPLC-PDA chromatogram of a microscopic sample removed from a yellow inlay (S4) appeared to simply contain the resin's characteristic flavonoids, while neither *Escobedia scabrifolia* nor other yellow dyes—references of which have been also examined for comparison—were detected. However, close inspection of the data revealed that the peak of luteolin, relatively to the other two flavonoids present, was more intense in S4 (yellow decoration) than in the *Elaeagia* reference resin and S5 (untinted resin), which might cautiously be interpreted as indicative of the use of a luteolin-based yellow dye (Additional file 3: Figure S3). However, it was not possible to confirm this hypothesis as, in this case, a decision was made to avoid removal of another sample to preserve the object's integrity.

Identification of the gourd's blues and blacks, found both in areas of the decoration as well as in all the dark outlines of the inlaid figures, was relatively straightforward. Humboldt described the blue as "*made by dissolving indigo in a lot of water and heating the resin a little*" and the black as produced "*with a large quantity of indigo, heating it a lot*" [14]. As per his account, an indigotin-based dye, likely indigo, was detected by FORS due to the observation of an apparent absorbance maximum at 660 nm in the blue inner rim and in some of the decorations' outlines (Fig. 6b). This identification was further supported by the Raman spectra of a selection of blue and black elements accessible for analysis with the system used, in which the main band of indigotin arises at 1572 cm^{-1} [81].

While Humboldt did not specify the pigments supposedly employed for green areas in *barniz de Pasto* objects, he did mention artisans chewing a ball of blue (presumably indigo) and one of yellow (an organic yellow, likely from *Escobedia scabrifolia*) to produce green. In accordance with his description, IRRFC and UVRFC images of the gourd's green background suggested the presence of indigotin, which showed as red in the former, and of

Fig. 7 **a** UVRFC and **c** IRRFC images of the gourd's bottom, in which organic yellows and indigotin, respectively, show as red. A visible light image **b** is also provided for comparison

organic yellows, which showed as red in the latter (Fig. 7) [78–80]. The use of indigotin was conclusively confirmed by FORS (Fig. 6c) and Raman spectroscopy, while the yellow component, in this case, was not analyzed micro-invasively, although it is safe to assume that it could be the same colorant found in the yellow and golden areas of the gourd's decoration.

Decoration stratigraphy

While a wealth of information on the materials of the gourd was gathered using non-invasive techniques, removal of five cross section samples followed by examination of their stratigraphy with optical microscopy and SEM/EDS was crucial to shed light both on the object's manufacturing techniques and on the exact composition of its metallic elements, primarily the silver leaf. Detailed results regarding the layer structure of an artifact created with the *barniz de Pasto* technique are reported in the following section for the first time.

Polarized light and UV photographs of a first sample (S1) (Fig. 8a), taken from the gourd's green background at a location on the neck where a large portion of the decoration had detached, revealed a stratigraphy that includes, from the bottom up, three layers of resin of different colors, one orange, one yellow, and one green. SEM/EDS enabled detection of a silver leaf of 1-µm thickness between the yellow and green resin layers. This leaf is composed of nearly pure silver with traces of copper and mercury, as well as low amounts of chlorine, possibly indicating the presence of silver chlorides as degradation products.

Another sample (S2) (Fig. 8b) collected from the red inner border showed that, unlike the green resin layer, the red layer directly on top of the silver leaf in this area is extremely thin, measuring about 20 µm versus the over 100 µm of each of the three layers of tinted resin observed in the previous sample.

Interestingly, a third sample (S3) (Fig. 8c) removed from one of the gold and blue triangles on the gourd's inner rim showed the presence of two distinct silver leaves: the first is located in the lowermost portion of the cross section, lying underneath a blue resin layer that ranges between 10 and 20 µm of thickness; the other, whose degradation is clearly indicated by the presence of silver chlorides, is sandwiched between a superficial, 3 to 15-µm golden-white layer, mostly composed of a mixture of calomel and lead white, and a dark yellow mopa mopa layer of about 100-µm thickness. It is worth noting that the absence of gold in the EDS spectra supports Humboldt's description of golden colors in *barniz de Pasto* objects as tinted resin over silver leaf; however, the actual stratigraphy of the gourd's golden areas as revealed by scientific analysis appears to be significantly more complex than he believed it to be.

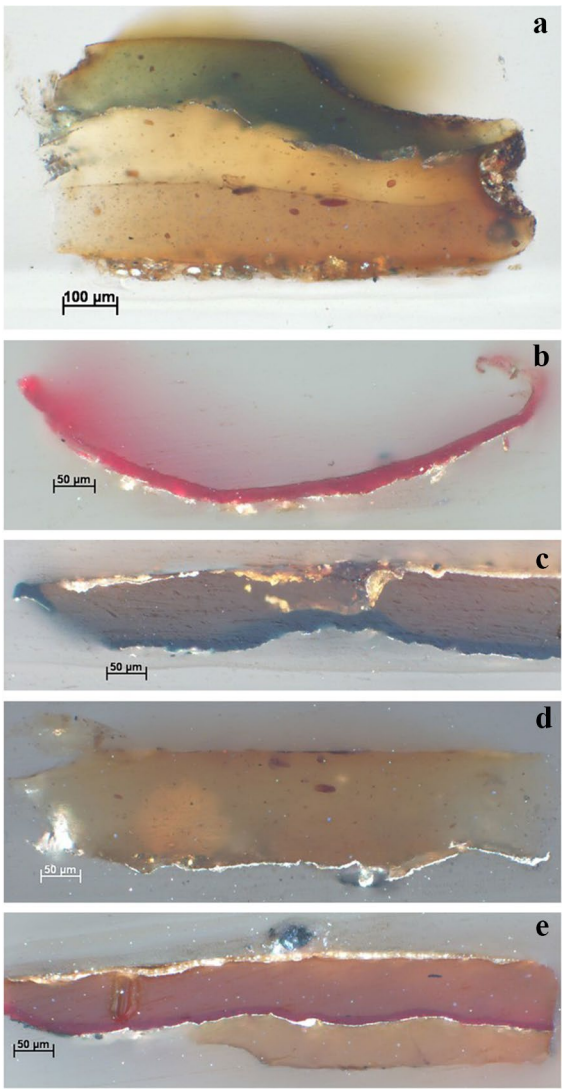

Fig. 8 Cross sections **a** S1, **b** S2, **c** S3, **d** S4, and **e** S6, removed from various areas of the gourd's decoration, revealing the complexity of the *barniz de Pasto* technique

A yellow sample (S4) (Fig. 8d) taken from an existing loss in one of the leaves near the unicorn figure was characterized by a relatively simple structure, with a layer of yellow-tinted resin of 120 to 150-µm thickness lying on top of the 1-µm thick silver leaf.

Finally, an additional sample (S6) (Fig. 8e), removed from one of the crescent moons on the red border that frame the quadrants of the gourd's decoration, displays a more intricate stratigraphy that includes multiple layers. Polarized light and UV photographs, as well as BSE images (Fig. 9a) and EDS data (Fig. 9b–d),

revealed, from the bottom up, the following structure: a yellow layer of mopa mopa resin of about 50-µm thickness; a 1-µm thick silver leaf, generally well preserved except for a blackened, exposed portion at left that contains degradation products mainly in the form of silver sulfides; a thin layer of red-tinted resin measuring approximately 20 µm, similar to that observed in sample S2; another 50-µm thick layer of mopa mopa that appears to have been tinted orange; a second silver leaf, with associated silver chlorides indicating, again, a possible degradation process; and the uppermost layer, with an abundance of 2-µm calomel particles dispersed in a resin layer of 10-µm average thickness. Silver(I) sulfide (Ag_2S) is reported as one of the most common advanced degradation products of silver, typically found in the form of monoclinic crystals known to mineralogists as acanthite and arising from a corrosion phenomenon referred to as tarnishing [82]. The presence of silver sulfide in a number of white-, silver-, and golden-looking details of the gourd's decoration was also confirmed with Raman analysis, due to the detection of broad bands at 92 and 241 cm^{-1} [82], respectively assigned to the Ag lattice vibrational modes and Ag–S stretching modes.

Radiocarbon dating

Preliminary hypotheses on dating the HSML gourd were based solely on stylistic considerations and on the visual examination of its decorative features. In particular, the finely detailed decoration, along with the inclusion of religious motifs and figurative elements from European early modern manuscripts as well as local flora and fauna, appear to be indicative of earlier artifacts dating to before ca. 1650. However, European artistic fashions continued to be popular in South America long after they ceased to be practiced in Europe; therefore, radiocarbon dating was performed, despite needing a 5-mg sample of gourd substrate (S7). Results showed date ranges of 1492–1644 C.E. with a 95% probability and 1522–1638 C.E. with 68% probability, which conclusively places the object under study in the early *barniz de Pasto* period.

Conclusions

In addition to providing tremendous insight into the variety of materials and manufacturing techniques used in the HSML lacquered gourd, the current study has unveiled a wealth of technical information regarding the so far poorly studied *barniz de Pasto* practice. Scientific analysis enabled us to unequivocally classify the gourd as a *barniz de Pasto* object by characterizing the resin employed for its decoration as *Eleaegia pastoensis*. The color palette was found to include some of

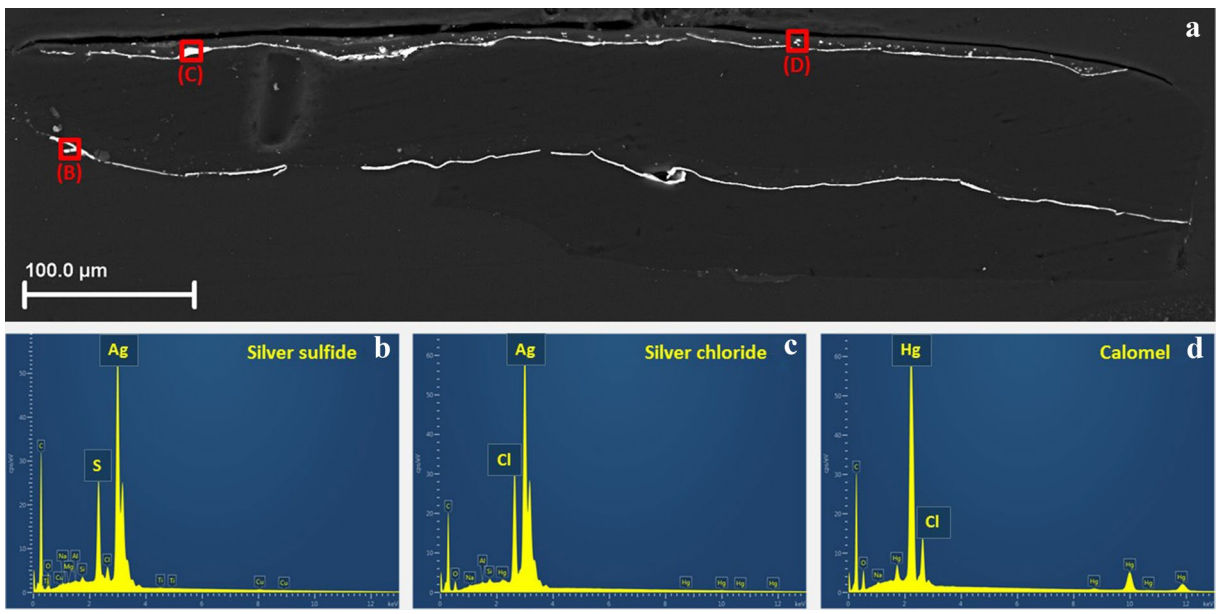

Fig. 9 **a** BSE image of cross section S6, removed from one of the crescent moons on the red border that frame the gourd's decoration quadrants. **b**–**d** EDS spectra of three areas of the cross section corresponding to the marked red squares, highlighting, respectively, the presence of silver sulfides, silver chlorides, and calomel

the pigments listed by Humboldt in his account, such as indigo, but also comprises other materials, such as cochineal for red and calomel, sometimes in combination with lead white, for whites and grays. Interestingly, the identification of calomel in some of the gourd's decorations and outlines supports the recent, but still rare, findings of mercury(I) chloride used deliberately as a white pigment in a *barniz de Pasto* table cabinet from the Victoria and Albert Museum [33] and in other artifacts from the Fitzwilliam Museum [67], conclusively demonstrating that this material was more commonly employed in works of art and cultural heritage objects than initially believed. Examination of the object's stratigraphy in five microscopic cross section samples, including up to six layers, revealed the incredible complexity of the *barniz de Pasto* technique, in which an extremely thin silver leaf is typically applied on top of a layer of untinted resin, and covered with a variable number of dyed resin layers whose thickness ranges from 10 to over 150 μm. Finally, radiocarbon dating, confirming for the gourd a pre-1650 date, supported stylistic observations that had placed this object in the early *barniz de Pasto* period. While the study of materials in Spanish American art is still in its infancy, the current work clearly reveals the extremely sophisticated knowledge that indigenous artisans had of botany, mineralogy, and metallurgy, greatly contributing to the current scholarship of a vibrant culture and its artistic traditions.

From a conservation standpoint, the research on materials characterization contained in this article represents the first step in the process of establishing conservation protocols for *barniz de Pasto* objects. While the condition of *barniz de Pasto* artifacts in the HSML collection is good, with both the decoration and structure assessed as stable, a correct identification of their materials and techniques was an institutional priority aiming to address two basic conservation issues, namely delamination and cleaning. Where delamination has occurred, it has often been caused by movement in the wooden or vegetal substrates as a result of changes in humidity. Losses on the gourd in this study, for example, are concentrated in close proximity to the main vertical crack and around the four bored holes, originally meant for a stand, in the rounded base. Prized as they were, *barniz de Pasto* objects have been traditionally repaired with materials such as shellac and wax, which often overlay the original decoration and are absorbed into the substrate, making it difficult to remove as well as attracting dirt. Therefore, the development of materials-guided cleaning guidelines is a key objective of further research in this field. In addition, one important corollary of the present work for conservators is that the mopa mopa resin appears to be resistant to most solvents, which will allow for greater options in terms of conservation treatments.

Supplementary information

Supplementary information accompanies this paper at https://doi.org/10.1186/s40494-020-00449-1.

Additional file 1: Figure S1. Photograph of the *Elaeagia pastoensis* L. E. Mora plant. Photograph by Isau Huamantupa, Cerros de Kampankis, Amazonas, Peru, August 2011. © Tropicos. Missouri Botanical Garden.

Additional file 2: Figure S2. (A) HPLC-PDA chromatogram at $\lambda = 490$ nm obtained upon extraction in 4% BF_3 in MeOH of sample S2, i.e. a scraping of red decoration from the gourd's inner neck, compared with (B) a chromatogram acquired in the same conditions from reference carminic acid. Compounds identified in both chromatograms include carminic acid and two of its methylated derivatives.

Additional file 3: Figure S3. (A) HPLC-PDA chromatogram at $\lambda = 350$ nm obtained upon extraction in 4% BF_3 in MeOH of sample S4, i.e. a scraping of yellow decoration from a leaf near the unicorn figure, compared with chromatograms acquired in the same conditions from (B) a reference sample of *Elaeagia pastoensis* boiled resin and (C) the extract of *Escobedia scabrifolia* roots. Compounds identified in sample S4 include luteolin, apigenin, and luteolin monomethylether or related derivative; luteolin appears to be present in slightly higher relative amounts in sample S4 than in the *Elaeagia* reference, cautiously suggesting the use of a luteolin-based dye.

Abbreviations

XRF: X-ray fluorescence spectroscopy; IRRFC: Infrared reflectance false color; UVRFC: Ultraviolet reflectance false color; FORS: Fiber optics reflectance spectroscopy; SERS: Surface-enhanced Raman spectroscopy; SEM/EDS: Scanning electron microscopy with energy-dispersive X-ray spectroscopy; HPLC-PDA: High-performance liquid chromatography with photodiode array detector; Py-GC/MS: Pyrolysis-gas chromatography/mass spectrometry.

Acknowledgements

The authors would like to acknowledge Marina Ruiz Molina, paper conservator at The Met, for helping with multiband imaging of the gourd; Marc Vermeulen, former Met fellow, for his assistance with IRRFC and UVRFC imaging; Nobuko Shibayama, scientist at The Met, for her precious guidance with HPLC-PDA analysis; and Deborah Schorsch, objects conservator at The Met, for contributing to this study with X-radiography. The authors are also grateful to Richard Cruz and Greg Hodgins from the Accelerator Mass Spectrometry Laboratory, University of Arizona (Tucson, Arizona), for conducting radiocarbon dating. MK would like to thank her colleagues at HSML, particularly Dr. Mitchell Codding, Dr. John O'Neill, and Hélène Fontoira Marzin. Many thanks are also due to Richard Newman, Museum of Fine Arts (Boston, Massachusetts), and Emily Kaplan, Smithsonian NMAI (Washington DC), for their generosity and their research.

Authors' contributions

FP and EB performed XRF and FORS analysis and data interpretation, and assisted with multiband imaging and X-radiography. FP removed samples, prepared the cross sections, carried out optical microscopy, Raman, SERS, Py-GC/MS, and HPLC-PDA analysis and data interpretation, and drafted the manuscript. EB conducted SEM/EDS analysis and data interpretation. MK provided art historical as well as geographical context, and supported the scientific work. All authors read and approved the final manuscript.

Funding

This research was made possible by the Network Initiative for Conservation Science (NICS), a Metropolitan Museum of Art program. Support for NICS was provided by a grant from The Andrew W. Mellon Foundation.

Availability of data and materials

All data generated during this study are included in this published article or are available from the corresponding author on reasonable request.

Competing interests
The authors declare that they have no competing interests.

Author details
[1] Department of Scientific Research, The Metropolitan Museum of Art, 1000 Fifth Avenue, New York, NY 10028, USA. [2] Department of Conservation, Hispanic Society Museum & Library, 613 West 155th Street, New York, NY 10032, USA.

Received: 21 July 2020 Accepted: 5 October 2020
Published online: 19 October 2020

References

1. Katz M. Local color: the visual analysis of a South American colonial lacquered gourd in the collection of the Hispanic Society Museum and Library. In: AIC Wooden Artifacts Group Postprints. Uncasville, Connecticut; 2019. p. 19–27.
2. Whitaker TW. Lagenaria: a pre-Columbian cultivated plant in the Americas. S J Anthropol. 1948;4(1):49–68.
3. Friedmann NS. Mopa-mopa o barniz de Pasto: los marcos de la iglesia bogotana de Egipto. In: Lecciones barrocas: pinturas sobre la vida de la Virgen de la Ermita de Egipto; 1990. p. 40–53.
4. Tropicos. Missouri Botanical Garden. https://www.tropicos.org/home. Accessed 4 Sept 2020.
5. Pearlstein EJ, Kaplan E, Howe E, Levinson J. Technical analyses of painted Inka and colonial qeros. In: Objects Specialty Group Postprints, Vol. 6. Washington DC: The American Institute for Conservation of Historic & Artistic Works; 1999–2000. p. 94–111.
6. Newman R, Kaplan E, Derrick M. Mopa mopa: scientific analysis and history of an unusual South American resin used by the Inka and artisans in Pasto. Colombia J Am Inst Conserv. 2015;54(3):123–48.
7. Mora-Osejo LE. El barniz de Pasto. Caldasia. 1977;5–31.
8. Katz M. Colonial Spanish American lacquered objects in the collection of the Hispanic Society of America. In: AIC Wooden Artifacts Group Postprints. Montreal, Quebec, Canada; 2016. p. 37–48.
9. de Escobar J. Memorial que la Fray Geronimo Descobar predicador de la orden de Sant Agustin al Real Consejo de Indias de lo que toca a la provincia de Popayan (1582). In: Tovar Pinzón H, editor. Relaciones y visitas a los Andes. Siglo XVI. Santafé de Bogotá: Colcultura/Instituto de Cultura Hispanica; 1993. p. 405.
10. Fernandez de Piedrahita L. Historia General de las Conquistas del Nuevo Reyno de Granada. Antwerp: JB Verdussen; 1688. p. 360.
11. Simon P. Noticias Historiales de las conquistas de Terre Firme en las Indias Occidentales. Ediciones de la Revista Bolivar, Ministerio de Educacion Nacional. 1953;47(6).
12. de Santa Gertrudis J. Maravillas de la naturaleza. 2 Vols. Bogota: Empresa Nacional de Publicaciones; 1956. p. 76–7.
13. Boussingault JB. Sobre la composicion del barniz de los Indios de pasto. In: Viajes cientificos a los Andes ecuatoriales: ó Coleccion de memorias sobre física, química é historia natural. Lasserre. Paris: Libreria Castellana; 1849. p 116–119.
14. Humboldt A. Sobre el barniz de Pasto. In: Alexander Humboldt en Colombia. Extractos de sus diarios. Bogotá, Colombia: Publicismo y Ediciones, Academia Colombiana de Ciencias Exactas Físicas y Naturales; 1982.
15. Seldes AM, Burucúa JE, Maier MS, Abad G, Jáuregui A, Siracusano G. Blue pigments in South American painting (1610–1780). J Am Inst Conserv. 1999;38(2):100–23.
16. Seldes A, Burucúa JE, Siracusano G, Maier MS, Abad GE. Green, yellow, and red pigments in South American painting, 1610–1780. J Am Inst Conserv. 2002;41(3):225–42.
17. Gómez BA, Parera SD, Siracusano G, Maier MS. Integrated analytical techniques for the characterization of painting materials in two South American polychrome sculptures. e-PS. 2010;7:1–7.
18. Fazio AT, Papinutti L, Gómez BA, Parera SD, Romero AR, Siracusano G, Maier MS. Fungal deterioration of a Jesuit South American polychrome wood sculpture. Int Biodeter Biodegr. 2010;64(8):694–701.
19. Tomasini EP, Landa CR, Siracusano G, Maier MS. Atacamite as a natural pigment in a South American colonial polychrome sculpture from the late XVI century. J Raman Spectrosc. 2013;44(4):637–42.
20. Marte F, Careaga VP, Mastrangelo N, de Faria DL, Maier MS. The Sibyls from the church of San Pedro Telmo: a micro-Raman spectroscopic investigation. J Raman Spectrosc. 2014;45(11–12):1046–51.
21. Tomasini EP, Gómez B, Halac EB, Reinoso M, Di Liscia EJ, Siracusano G, Maier MS. Identification of carbon-based black pigments in four South American polychrome wooden sculptures by Raman microscopy. Herit Sci. 2015;3(1):19.
22. Tomasini E, Rodríguez DC, Gómez BA, de Faria DL, Landa CR, Siracusano G, Maier MS. A multi-analytical investigation of the materials and painting technique of a wall painting from the church of Copacabana de Andamarca (Bolivia). Microchem J. 2016;128:172–80.
23. Tomasini EP, Marte F, Careaga VP, Landa CR, Siracusano G, Maier MS. Virtuous colours for Mary. Identification of lapis lazuli, smalt and cochineal in the Andean colonial image of Our Lady of Copacabana (Bolivia). Philos Trans R Soc A. 2016;374(2082):20160047.
24. Kriss D, Howe E, Levinson J, Rizzo A, Carò F, DeLeonardis L. A material and technical study of Paracas painted ceramics. Antiquity. 2018;92(366):1492–510.
25. Levy IK, Tauil RN, Valacco MP, Moreno S, Siracusano G, Maier MS. Investigation of proteins in samples of a mid-18th century colonial mural painting by MALDI-TOF/MS and LC-ESI/MS (Orbitrap). Microchem J. 2018;143:457–66.
26. Tomasini EP, Cárcamo J, Rodríguez DM, Careaga V, Gutiérrez S, Landa CR, Sepúlveda M, Guzman F, Pereira M, Siracusano G, Maier MS. Characterization of pigments and binders in a mural painting from the Andean church of San Andrés de Pachama (northernmost of Chile). Herit Sci. 2018;6(1):61.
27. Pozzi F, Arslanoglu J, Cesaratto A, Skopek M. How do you say "Bocour" in French? The work of Carmen Herrera and acrylic paints in post-war Europe. J Cult Herit. 2019;35:209–17.
28. Mahon D, Centeno SA, Smieska L. Cristóbal de Villalpando's Adoration of the Magi: a discussion of artist technique. Latin Am Vis Cult. 2019;1(2):113–21.
29. Portell JD. Colored glazes on silver-gilded surfaces. Stud Conserv. 1992;37(sup1):116–8.
30. Howe E, Kaplan E, Newman R, Frantz JH, Pearlstein E, Levinson J, Madden O. The occurrence of a titanium dioxide/silica white pigment on wooden Andean qeros: a cultural and chronological marker. Herit Sci. 2018;6:41.
31. Newman R, Derrick M. Painted qero cups from the Inka and Colonial periods in Peru: an analytical study of pigments and media. In: MRS online proceedings library archive. 2002;712.
32. Curley AN, Thibodeau AM, Kaplan E, Howe E, Pearlstein E, Levinson J. Isotopic composition of lead white pigments on qeros: implications for the chronology and production of Andean ritual drinking vessels during the colonial era. Herit Sci. 2020;8:72.
33. Burgio L, Melchar D, Strekopytov S, Peggie DA, Di Crescenzo MM, Keneghan B, Najorka J, Goral T, Garbout A, Clark BL. Identification, characterisation and mapping of calomel as 'mercury white', a previously undocumented pigment from South America, and its use on a barniz de Pasto cabinet at the Victoria and Albert Museum. Microchem J. 2018;143:220–7.
34. Aceto M, Agostino A, Fenoglio G, Idone A, Gulmini M, Picollo M, Ricciardi P, Delaney JK. Characterisation of colourants on illuminated manuscripts by portable fibre optic UV–visible-NIR reflectance spectrophotometry. Anal Methods. 2014;6(5):1488–500.
35. Cesaratto A, Leona M, Pozzi F. Recent advances on the analysis of polychrome works of art: SERS of synthetic colorants and their mixtures with natural dyes. Front Chem. 2019;7(105):1–12.
36. Cesaratto A, Leona M, Pozzi F. The cultural meanings of color: Raman spectroscopic studies of red, pink, and purple dyes in late Edo and early Meiji period prints. In: Vandenabeele P, Edwards H, editors. Raman Spectroscopy in archaeology and art history, vol. 2. London: Royal Society of Chemistry; 2018. p. 271–288.
37. Leona M. Microanalysis of organic pigments and glazes in polychrome works of art by surface-enhanced resonance Raman scattering. PNAS. 2009;106(35):14757–62.

38. Kirby J, White R. The identification of red lake pigment dyestuff and a discussion of their use. Natl Gallery Tech Bull. 1996;17:56–80.
39. Chiavari G, Fabbri D, Prati S. Effect of pigments on the analysis of fatty acids in siccative oils by pyrolysis methylation and silylation. J Anal Appl Pyrol. 2005;74:39–44.
40. Insuasty B, Argoti JC, Altarejos J, Cuenca G, Chamorro E. Caracterización fisicoquímica preliminar de la resina del mopa-mopa (*Elaeagia pastoensis* Mora), *barniz de Pasto*. Scientia et technica. 2007;13(33):365–8.
41. Creixell R. Entre el viejo y el Nuevo Mundo: el escritorio de barniz de pasto de la colección de artes decorativas de The Hispanic Society of America. Res Mobilis: revista internacional de investigación en mobiliario y objetos decorativos. 2014;3(3):119–31.
42. Spring M, Grout R. The blackening of vermilion: an analytical study of the process in paintings. Natl Gallery Tech Bull. 2002;23:50–61.
43. Keune K, Boon JJ. Analytical imaging studies clarifying the process of the darkening of vermilion in paintings. Anal Chem. 2005;77(15):4742–50.
44. Radepont M, de Nolf W, Janssens K, Van der Snickt G, Coquinot Y, Klaassen L, Cotte M. The use of microscopic X-ray diffraction for the study of HgS and its degradation products corderoite (α-$Hg_3S_2Cl_2$), kenhsuite (γ-$Hg_3S_2Cl_2$) and calomel (Hg_2Cl_2) in historical paintings. J Anal Atom Spectrom. 2011;26(5):959–68.
45. Dominguez-Vidal A, de la Torre-Lopez MJ, Rubio-Domene R. In situ noninvasive Raman microspectroscopic investigation of polychrome plasterworks in the Alhambra. Analyst. 2012;137(24):5763–9.
46. Vermeulen M, Sanyova J, Janssens K. Identification of artificial orpiment in the interior decorations of the Japanese tower in Laeken, Brussels, Belgium. Herit Sci. 2015;3(1):9.
47. Nevin A. Pigment alteration. In: The encyclopedia of archaeological sciences. 2018;10:1–4.
48. Sodo A, Tortora L, Biocca P, Casanova Municchia A, Fiorin E, Ricci MA. Raman and time of flight secondary ion mass spectrometry investigation answers specific conservation questions on Bosch painting Saint Wilgefortis Triptych. J Raman Spectrosc. 2019;50(2):150–60.
49. Urdang G. The early chemical and pharmaceutical history of calomel. Chymia. 1948;1:93–108.
50. Copan L, Fowles J, Barreau T, McGee N. Mercury toxicity and contamination of households from the use of skin creams adulterated with mercurous chloride (calomel). Int J Environ Res Pub Health. 2015;12(9):10943–54.
51. Cavallo G, de Ágredos Pascual ML. X-ray powder diffraction of mineral pigments and medicines from the 17th century pharmacy (Spezieria) Santa Maria della Scala in Rome. Italy Powder Diffr. 2018;33(4):270–8.
52. Takamatsu T. On Japanese pigments. Tokyo: Department of Science in Tokyo Daigaku; 1878.
53. Divers E. The manufacture of calomel in Japan. Am J Pharm (1835–1907). 1894: 232–243.
54. Swiderski RM. Calomel in America: mercurial panacea, war, song and ghosts. Irvine: Universal-Publishers; 2008.
55. Burger RL, Lane KE, Cooke CA. Ecuadorian cinnabar and the prehispanic trade in vermilion pigment: viable hypothesis or red herring? Lat Am Antiq. 2016;27(1):22–35.
56. Cooke CA, Balcom PH, Biester H, Wolfe AP. Over three millennia of mercury pollution in the Peruvian Andes. PNAS. 2009;106(22):8830–4.
57. Lacerda LD. Global mercury emissions from gold and silver mining. Water Air Soil Pollut. 1997;97(3–4):209–21.
58. Cooke CA, Balcom PH, Kerfoot C, Abbott MB, Wolfe AP. Pre-Colombian mercury pollution associated with the smelting of argentiferous ores in the Bolivian Andes. Ambio. 2011;40(1):18–25.
59. Brooks WE. Colombia mercury inventory 2011. Geol Colomb. 2012;37:15–50.
60. Cooke CA, Hintelmann H, Ague JJ, Burger R, Biester H, Sachs JP, Engstrom DR. Use and legacy of mercury in the Andes. Environ Sci Technol. 2013;47(9):4181–8.
61. Scott DA, Doughty DH, Donnan CB. Moche wallpainting pigments from La Mina, Jequetepeque, Peru. Stud Conserv. 1998;43:177–82.
62. Brooks WE, Piminchumo V, Suárez H, Jackson JC, McGeehin JP. Mineral pigments at Huaca Tacaynamo (Chan Chan, Peru). Bull de l'Institut français d'études andines. 2008;37(3):441–50.
63. Freire E, Acevedo V, Halac EB, Polla G, López M, Reinoso M. X-ray diffraction and Raman spectroscopy study of white decorations on tricolored ceramics from Northwestern Argentina. Spectrochim Acta Part A Mol Biomol Spectrosc. 2016;157:182–5.
64. Wright V, Pacheco G, Torres H, Huaman O, Watanave A, Zeballos-Velasquez EL, Suchomel MR, Suescun L, Moulin C, Sandoval PCM. Mural paintings in ancient Peru: the case of Tambo Colorado. Pisco Valley Sci Technol Archaeol Res. 2016;1(2):11–21.
65. Siracusano G. Pigments and power in the Andes: from the material to the symbolic in Andean cultural practices, 1500–1800. Barnett I, translator. London: Archetype Publications Ltd; 2011.
66. Kaplan E, Howe E, Pearlstein E, Levinson J. The qero project: conservation and science collaboration over time. In: Research and Technical Studies Postprints, American Institute for Conservation. 2012;3:1–24.
67. Crippa M, Legnaioli S, Kimbriel C, Ricciardi P. New evidence for the intentional use of calomel as a white pigment. J Raman Spectrosc. 2020. https://doi.org/10.1002/jrs.5876.
68. Pastoureau M. Red: the history of a color. Princeton: Princeton University Press; 2017.
69. Pearlstein E, Mackenzie M, Kaplan E, Howe E, Levinson J. Tradition and innovation. Cochineal and Andean keros. In: Padilla C, Anderson BC, Clark B, editors. A red like no other: how cochineal colored the world: an epic story of art, culture, science, and trade. New York: Skira Rizzoli; 2015.
70. Cardon D. Natural dyes. Sources, tradition, technology and science. London: Archetype Publications; 2007.
71. Fonseca B, Patterson CS, Ganio M, MacLennan D, Trentelman K. Seeing red: towards an improved protocol for the identification of madder-and cochineal-based pigments by fiber optics reflectance spectroscopy (FORS). Herit Sci. 2019;7(1):92.
72. Anderson B. The world of cochineal. In: Padilla C, Anderson BC, Clark B, editors. A red like no other: how cochineal colored the world: an epic story of art, culture, science, and trade. New York: Skira Rizzoli; 2015.
73. Dupey GÉ. The materiality of color in pre-Columbian codices: insights from cultural history. Anc Mesoam. 2017;28(1):21–40.
74. Pennell FW. Escobedia: a neotropical genus of the Scrophularlaceae. Proc Acad Nat Sci Phila. 1931;83:411–26.
75. Bruni S, Guglielmi V, Pozzi F, Mercuri AM. Surface-enhanced Raman spectroscopy (SERS) on silver colloids for the identification of ancient textile dyes. Part II: pomegranate and sumac. J Raman Spectrosc. 2011;42(3):465–73.
76. García ÉD. The materiality of color in pre-Columbian codices: insights from cultural history. Anc Mesoam. 2017;28(1):21.
77. Garcia-Bucio MA, Maynez-Rojas MÁ, Casanova-González E, Cárcamo-Vega JJ, Ruvalcaba-Sil JL, Mitrani A. Raman and surface-enhanced Raman spectroscopy for the analysis of Mexican yellow dyestuff. J Raman Spectrosc. 2019;50(10):1546–54.
78. Dyer J, Tamburini D, O'Connell ER, Harrison A. A multispectral imaging approach integrated into the study of Late Antique textiles from Egypt. PLoS ONE. 2018;13(10):e0204699.
79. Tamburini D, Dyer J. Fibre optic reflectance spectroscopy and multispectral imaging for the non-invasive investigation of Asian colourants in Chinese textiles from Dunhuang (7th–10th century AD). Dyes Pigm. 2019;162:494–511.
80. Vermeulen M, Müller EMK, Leona M. Non-invasive study of the evolution of pigments and colourants use in 19th century ukiyo-e. Arts of Asia. 2020;50(2).
81. Vandenabeele P, Moens L. Micro-Raman spectroscopy of natural and synthetic indigo samples. Analyst. 2003;128(2):187–93.
82. Martina I, Wiesinger R, Jembrih-Simbürger D, Schreiner M. Micro-Raman characterisation of silver corrosion products: instrumental set up and reference database. E-Preserv Sci. 2012;9:1–8.

Publisher's Note